1521-0111/99/4/277–285$35.00
MOLECULAR PHARMACOLOGY

https://doi.org/10.1124/molpharm.120.000117
Mol Pharmacol 99:277–285, April 2021

A Potential Role for SerpinA3N in Acetaminophen-Induced Hepatotoxicity

Melanie Tran, Jianguo Wu, Li Wang, and Dong-Ju Shin

Department of Physiology and Neurobiology, University of Connecticut, Storrs, Connecticut (M.T., J.W., D.-J.S.) and Department of Internal Medicine, Section of Digestive Diseases, Yale University, New Haven, Connecticut (L.W.)

Received July 17, 2020; accepted December 31, 2020

ABSTRACT

Acetaminophen (APAP) is a commonly used pain and fever reliever but is also the most frequent cause of drug-induced liver injury. The mechanism pertaining acetaminophen toxicity has been well documented, whereas mechanisms of hepatotoxicity are not well established. Serine (or cysteine) peptidase inhibitor, clade A, member 3N (SerpinA3N), a serine protease inhibitor, is synthesized in the liver but the role of SerpinA3N in relation to APAP-induced liver injury is not known. Wild-type and hepatocyte-specific SerpinA3N knockout (HKO) mice were injected intraperitoneally with a single dose of PBS or APAP (400 mg/kg) for 12 hours, and markers of liver injury, cell death, and inflammation were assessed. SerpinA3N expression was highly induced in mice with APAP overdose. SerpinA3N HKO mice had diminished liver injury and necrosis as shown by lower alanine aminotransferase and interleukin-6 levels, accompanied by suppressed inflammatory cytokines and reduced neutrophil infiltration. The reduced oxidative stress was associated with enhanced antioxidant enzyme capabilities. Taken together, hepatocyte SerpinA3N deficiency reduced APAP-induced liver injury by ameliorating inflammation and modulating the 5′ AMP-activated protein kinase–unc-51-like autophagy activating kinase 1 signaling pathway. Our study provides novel insights into a potential role for SerpinA3N in APAP-induced liver injury.

SIGNIFICANCE STATEMENT

Our studies indicate that serine (or cysteine) peptidase inhibitor, clade A, member 3N (SerpinA3N) may have a pathophysiological role in modulating acetaminophen (APAP)-induced liver injury. More specifically, mice with hepatic deletion of SerpinA3N suppressed inflammation and liver injury to reduce APAP-induced hepatotoxicity. Controlling the inflammatory response offers possible approaches for novel therapeutics; therefore, understanding the pathophysiological role of SerpinA3N in inducing liver injury may add to the development of more efficacious treatments.

Introduction

Drug-induced liver injury (DILI) is a major cause of acute liver failure, accounting for over half of the overdose cases reported in the United States. Acetaminophen (APAP; N-acetyl-*p*-aminophenol) is a well-known hepatotoxin and is the most commonly used painkiller for treating mild to moderate pain, but an overdose can result in hepatotoxicity in humans and mouse models (McGill and Jaeschke, 2013; Ramachandran and Jaeschke, 2018; Yan et al., 2018). However, incomplete understanding of the mechanism pertaining the pathogenesis of DILI has limited the development of therapeutic strategies for patients with APAP overdose.

A wealth of data has demonstrated that drug-induced liver injury is induced through several mechanisms, including inflammatory response, oxidative stress, and apoptosis (McGill and Jaeschke, 2013; Ni et al., 2016; Ramachandran and Jaeschke, 2018; Yan et al., 2018). The key mechanism of hepatotoxicity is the metabolism of APAP by cytochrome P450 enzymes, which generates N-acetyl-p-benzoquinone imine (NAPQI), a reactive metabolite in the pericentral zone of the liver. The formation of excess NAPQI in the cell depletes cellular glutathione (GSH), an intracellular antioxidant, which impairs redox balance, resulting in the formation of protein adducts that compromise multiple cellular functions. Administration of N-acetyl cysteine at the early phase restores intracellular glutathione levels and scavenge NAPQI to protect against liver injury. However, many patients present only after this early phase has passed, and there are no treatments available to prevent liver injury in subsequent phases of pathogenesis.

Serine (or cysteine) peptidase inhibitor, clade A, member 3N (SerpinA3N), also referred to as α-1-antichymotrypsin, belongs

This work was supported by National Institutes of Health National Institute of Alcohol Abuse and Alcoholism [Grant R01AA026322] (to D.-J.S.). M.T. was supported by an American Heart Association Postdoctoral Fellowship [18POST33960183].
https://doi.org/10.1124/molpharm.120.000117.
This article has supplemental material available at molpharm.aspetjournals.org.

ABBREVIATIONS: ALT, alanine transaminase; AMPK, 5′ AMP-activated protein kinase; APAP, acetaminophen; AST, aspartate aminotransferase; ATG, autophagy related gene; CXCL, chemokine (C-X-C motif) ligand; DILI, drug-induced liver injury; GPX1, glutathione peroxidase 1; GSH, glutathione; HKO, hepatocyte-specific SerpinA3N knockout; HMGB, high motility group box; IL, interleukin; JNK, c-Jun N-terminal kinase; LC3, light chain; MDA, malondialdehyde; mTOR, mammalian target of rapamycin; NAPQI, N-acetyl-p-benzoquinone imine; NRF2, nuclear factor-like 2; PRDX1, peroxiredoxin-1; qPCR, quantitative polymerase chain reaction; SerpinA3N, serine (or cysteine) peptidase inhibitor; clade A, member 3N; SOD1, superoxide dismutase 1; TUNEL, terminal deoxynucleotidyl transferase-mediated digoxigenin-deoxyuridine nick-end labeling; ULK1, unc-51-like autophagy activating kinase 1; WT, wild type.

to the serpin family of protease inhibitors (Horvath et al., 2005; Aslam and Yuan, 2020). It is mainly synthesized by hepatocytes and is released in response to early inflammation. Serpins primarily function by inhibiting their protease activity, although some may have a noninhibitory effect. In mice, there are 13 closely related members in clade A, each with differing tissue and protease specificity (Horvath et al., 2005). Moreover, several studies have indicated that serpinA3N is the murine ortholog of the human SerpinA3 (Morgan and Kalsheker, 1997; Kalsheker et al., 2002; Horvath et al., 2005). Elevated levels of SerpinA3 have been reported in several disease pathologies (Cao et al., 2018; Ko et al., 2018, 2019) with SerpinA3 expressed at high levels in liver cancers with potential roles in regulating apoptosis and invasiveness (Matsuzaki et al., 1981; Cao et al., 2018; Ko et al., 2018, 2019). Animal models have also shown a role for SerpinA3N in modulating wound healing (Hsu et al., 2014), neuropathic pain (Vicuña et al., 2015), muscle atrophy disease models (Tjondrokoesoemo et al., 2016; Gueugneau et al., 2018), neurodegenerative disease (Haile et al., 2015), and levels were increased in response to high fat feeding and leptin challenge (Waise et al., 2015; Dalby et al., 2018; Sergi et al., 2018). Importantly, no studies to date have explored the specific role of SerpinA3N on acute liver injury which remains elusive.

Our findings demonstrate that SerpinA3N was markedly induced in mice with APAP overdose, and SerpinA3N deficiency in hepatocytes can diminish APAP-induced liver injury and inflammation. Moreover, we identified a new pathway mediated by SerpinA3N which may provide fundamental insight for developing unique therapies to control DILI.

Materials and Methods

Animals. A SerpinA3N floxed breeding pair on a mixed C57BL/6J: 129S background (stock #027511) was purchased from the Jackson Laboratory (Bar Harbor, ME). Homozygous floxed SerpinA3N mice were crossed with Albumin-Cre mice using the Cre-LoxP system to generate hepatocyte-specific SerpinA3N knockout (HKO) mice. All mice used in the study were 12-week-old male mice. To induce liver injury, an in vivo mouse model of APAP (Sigma Aldrich, St. Louis, MO) overdose was used. APAP (400 mg/kg) was dissolved in prewarmed PBS (pH 7.4) prior to administration. Wild-type (WT) and SerpinA3N HKO mice were allocated to one of the two experimental groups: PBS or APAP. Mice were fasted for 12 hours to deplete any cellular glutathione that may be present before injected intraperitoneally with PBS or APAP (at 2, 4, and 12 hours). Food was given back to mice after the PBS or APAP treatment. Mice were killed by CO_2 asphyxiation at 2 and 4 hours (WT mice only for histology in Fig. 1B) or 12 hours (for WT and SerpinA3N HKO mice) after the injection, and blood and liver were collected. All animal experimental and care procedures were approved by the University of Connecticut Institutional Animal Care and Use Committee, and the study was performed in accordance with the National Institutes of Health guide for the care and use of laboratory animals.

Biochemical Analysis. Plasma aspartate aminotransferase (AST), alanine transaminase (ALT) (Point Scientific, Canton, MI), and liver glutathione (Abcam, Cambridge, MA) levels were measured calorimetrically following the manufacturer's instructions. Plasma interleukin (IL)-6 levels were detected by ELISA (Cayman Chemicals, Ann Arbor, MI), following the manufacturer's instructions. Levels of hepatic H_2O_2 were detected fluorometrically using an Amplex Red reagent (Thermo Fisher Scientific, Waltham, MA). Liver malondialdehyde (MDA) levels were measured using thiobarbituric acid reactive substances assay (Ohkawa et al., 1979).

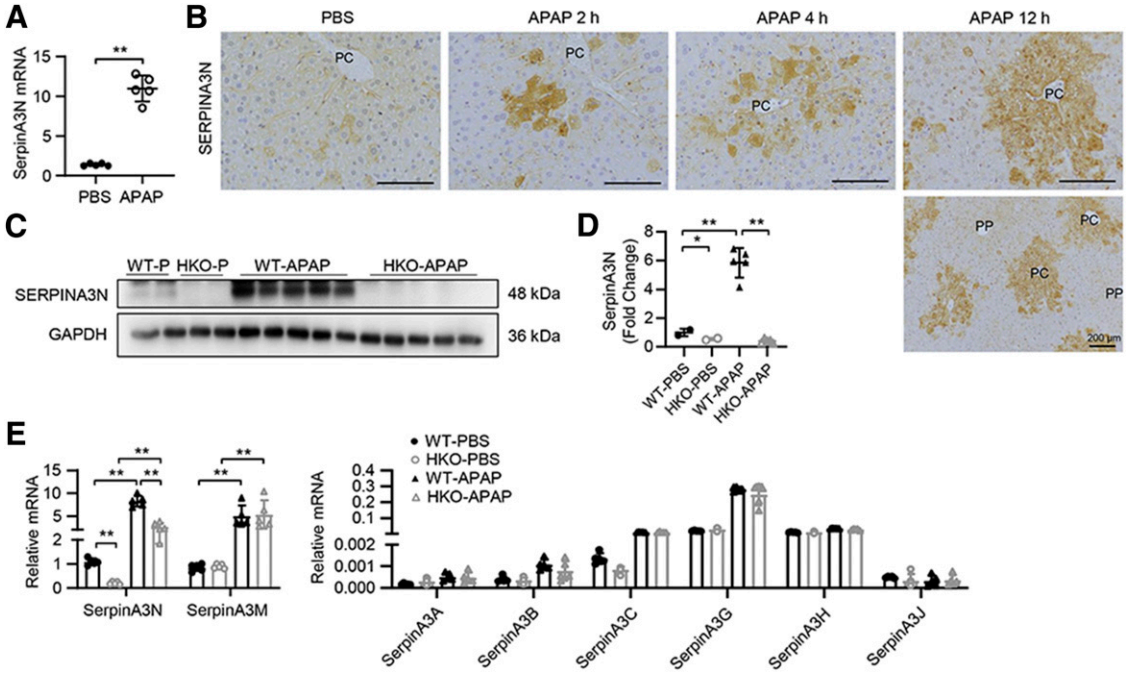

Fig. 1. SerpinA3N expression is markedly induced in mice with APAP overdose. (A) qPCR analysis of hepatic SerpinA3N mRNA. Student's *t* test was used to determine differences between two groups; $^{**}P < 0.01$ is considered statistically significant. (B) Representative immunohistochemistry images of SERPINA3N protein expression in livers of WT mice at 0, 2, 4, and 12 hours after APAP (400 mg/kg). Scale bar, 100 μm unless otherwise indicated. PP, periportal; PC, pericentral. (C) Protein expression of SerpinA3N in livers of WT and SerpinA3N HKO mice treated with PBS or APAP for 12 hours. GAPDH, glyceraldehyde-3-phosphate dehydrogenase. (D and E) qPCR analysis of *SerpinA3* family. Data are presented as means ± S.D., $n = 5$ per group. $^{*}P < 0.05$; $^{**}P < 0.01$ (considered statistically significant) after Bonferroni correction compared with drug treatment or with WT within the same drug treatment.

Immunoblotting Analysis. Snap frozen liver was homogenized in lysis buffer containing a cocktail of phosphatase and protease inhibitors. Equal amounts of protein were extracted and processed from five individual livers per group, and homogenates were pooled. Approximately 30 μg of protein was resolved by 10% or 12% SDS-PAGE. The specific primary antibodies used are listed in Supplemental Table 1. The following day, membranes were incubated in the corresponding secondary antibody for 1 hour. The secondary antibodies used were rabbit anti-goat (HAF109, LOT #XGD1018061, 1:1000; R&D Systems Inc.), goat anti-rabbit (#5160-2104, 1:10,000; Bio-Rad Laboratories, Hercules, CA), and goat anti-mouse (170-6516, LOT #L005680-A, 1:10,000; Bio-Rad Laboratories). Immunodetection was determined using the Pierce enhanced chemiluminescence detection system (Thermo Fisher Scientific), and images were obtained using the Image Quant LAS digital analyzer (GE Healthcare Life Sciences, Pittsburg, PA).

Gene Expression Analysis by Quantitative Polymerase Chain Reaction. Trizol reagent (Sigma-Aldrich) was used to extract total RNA from mouse livers, and then RNA was reverse transcribed with the iScript cDNA Synthesis Kit (Bio-Rad Laboratories). RNA was pooled from $n = 5$ per group or processed individually as described. Quantitative polymerase chain reaction (qPCR) was carried out using SYBR Green assay in Bio-Rad Cycler detection system. A PCR master mix containing specific primers was used, and mRNA expression was normalized to the internal reference gene hypoxanthine-guanine phosphoribosyl transferase. The threshold cycle (CT) was determined, and the relative gene expression was calculated as follows: fold change $2\Delta\Delta CT$. Primer sequences are listed in Supplemental Table 2.

Liver Histology. Liver samples were fixed in 10% formalin overnight, embedded in paraffin wax and sectioned at 4 μm. Liver sections were deparaffinized and then stained with H&E or used for immunohistochemistry. Liver sections were incubated with goat anti-SerpinA3N (AF4709, LOT #CBKW0216081, 1:100; R&D Systems Inc.) or rabbit anti-F4/80 antibody (ab100790, LOT #GR3229582-3, 1:100; Abcam) overnight at 4°C and then incubated with horseradish peroxidase–conjugated rabbit anti-goat (HAF109, LOT #XGD1018061, 1:500; R&D Systems) or goat anti-rabbit IgG secondary antibody (5160-2104, 1:500; Bio-Rad Laboratories) respectively, for 1 hour before detection with 3, 3′ diaminobenzidine tetrahydrochloride substrate (Vector Laboratories, Burlingame, CA) and counterstained with hematoxylin. Terminal deoxynucleotidyl transferase-mediated digoxigenin-deoxyuridine nick-end labeling (TUNEL)–positive cells were detected using the Dead End Calorimetric TUNEL assay (Promega, Madison, WI) according to the manufacturer's instructions. ImageJ (National Institutes of Health) software was used to quantify the necrotic area stained, and results were presented as percentage of necrotic area relative to the total area of view. About five randomly chosen fields per section were used for all analyses, and the number of mice quantified was indicated.

Statistical Analysis. Data are presented as means ± S.D. Analysis was performed using GraphPad Prism (Version 8; GraphPad Software Inc., La Jolla, CA). This study is largely exploratory, and accordingly the statistical analysis is descriptive. We performed a total of 196 comparisons from a sample comprised of 20 independent replicates. Our statistical analysis as detailed below does not adequately control for experiment-wise type 1 error. A Student's unpaired t test was used for comparisons between two groups. For comparisons of multiple groups, a one-way ANOVA was used to determine differences between genotype and drug treatment. Statistical significance was set at $^*P < 0.05$ unless otherwise indicated. To control for type 1 errors, a Bonferroni correction was conducted on some comparisons and a P value of less than 0.0063 (for Fig. 1E where eight comparisons were tested in the same samples), 0.017 (for Fig. 3, A–C where three comparisons were tested in the same samples), 0.0042 (for Fig. 3, D and F–H where twelve comparisons were tested in the same samples), 0.01 (for Fig. 4, C, D, and G where five comparisons were tested in the same samples), 0.0083 (for Fig. 4, A and E–G where six comparisons were tested in the same samples), and 0.025 (for Fig. 5 where two comparisons were tested in the same samples) were considered as statistically significant.

Results

SerpinA3N Expression Is Induced in Response to APAP-Induced Liver Injury. To determine whether SerpinA3N has a role in DILI, we examined the expression levels of SerpinA3N in mice with APAP overdose. We found a 10-fold induction of *SerpinA3N* mRNA (Fig. 1A) and elevated protein levels (Fig. 1, C and D) after APAP overdose in liver homogenates of WT mice compared with WT-PBS group. Additionally, histologic assessment in livers showed a concomitant increase in SerpinA3N expression with APAP at 2 and 4 hours (Fig. 1B), which was abundantly localized to the pericentral but not periportal regions of the liver at 12 hours (Fig. 1B). These results suggest that SerpinA3N may have a role in the pathogenesis of APAP-induced liver injury.

SerpinA3N is mainly synthesized by hepatocytes, and therefore we generated hepatocyte-specific SerpinA3N knockout mice. Protein and mRNA analysis revealed complete ablation of SerpinA3N expression in livers of HKO mice (Fig. 1, C–E) and APAP administration modestly increased SerpinA3N mRNA, but not protein levels in HKO mice (Fig. 1, C–E). The levels of other closely related genes of *SerpinA3* in the liver were assessed to determine whether any of these genes could be compensating for the lack of *SerpinA3N*. *SerpinA3M* expression was found to be relatively high in APAP-treated mice compared with PBS-treated mice (Fig. 1D), suggesting a possible increase in SerpinA3 member M to compensate for mostly ablated N levels. The expression of other SerpinA3 genes including A, B, C, G, H, and J was relatively low compared with SerpinA3N, but was similar among WT and HKO mice (Fig. 1E). Our results suggest that these SerpinA3 members may not play a prominent role in the pathogenesis of APAP-induced liver injury.

Hepatocyte SerpinA3N Deficiency Reduces APAP-Induced Necrosis and Liver Injury. Histologically, APAP destroys hepatocytes and induces centrilobular areas of necrosis within 2–6 hours (Hinson et al., 2010). Accordingly, H&E staining in livers of WT and HKO mice subjected to APAP overdose showed massive necrosis in the centrilobular but not pericentral region compared with mice treated with PBS (Fig. 2A). However, in Serpina3N HKO mice, there was reduced bridging necrosis compared with their WT counterparts (Fig. 2A), as indicated by the reduced percentage of necrotic area (Fig. 2B). The number of hepatocytes with TUNEL-positive cells were similar between WT and HKO mice after 12 hours of APAP overdose which were located around the centrilobular area (Fig. 2, A and B). Furthermore, active CASPASE-3 and CASPASE-8 were not detected in livers of WT and HKO mice with APAP overdose (Fig. 2C), suggesting that apoptosis may not be actively involved in mediating APAP-induced liver injury.

In accordance with our assessment of liver histology, APAP overdose resulted in a ~50-fold induction in plasma ALT and AST levels, which are surrogate markers for liver injury (Fig. 2D). However, SerpinA3N HKO mice had lower plasma ALT levels in response to APAP administration compared with WT-APAP mice (Fig. 2D). APAP overdose causes necrotic cell death which results in the immune system to release damage-associated molecular patterns, including

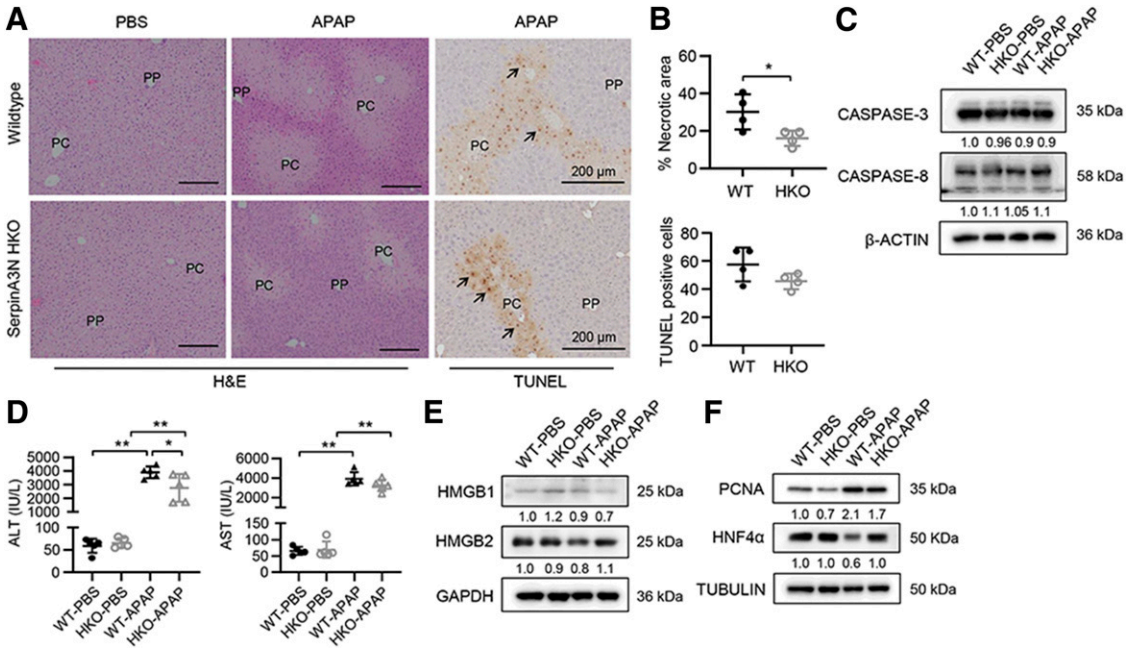

Fig. 2. Hepatocyte SerpinA3N deficiency diminishes APAP-induced liver injury and necrosis. (A) Representative images of H&E staining and TUNEL-positive cells in livers of WT and SerpinA3N HKO mice treated with a single dose of PBS or APAP (400 mg/kg) for 12 hours. Scale bar, 100 μm unless otherwise indicated. PP, periportal; PC, pericentral. (B) Quantification of percentage necrotic area and number of TUNEL-positive cells in WT-APAP and HKO-APAP mice. Data are presented as means ± S.D., $n = 4$ to 5 per group. Student's t test was used to determine differences between two groups; $P < 0.05$ is considered statistically significant. (C) Immunoblotting for CASPASE-3, CASPASE-8, and the respective loading control, β-ACTIN, in livers of WT and HKO mice. (D) Plasma ALT and AST levels. (E) Immunoblotting for HMGB1, HMGB2, and loading control glyceraldehyde-3-phosphate dehydrogenase (GAPDH) in livers of WT and HKO mice. (F) Immunoblotting for hepatocyte nuclear factor 4-alpha (HNF4α), proliferating cell nuclear antigen (PCNA), and loading control TUBULIN in livers of WT and HKO mice. *$P < 0.05$; **$P < 0.01$ (considered statistically significant) after Bonferroni correction compared with drug treatment.

high motility group box (HMGB)-1 and HMGB2. In keeping with the increased APAP-induced liver injury, HMGB1 protein levels were diminished in HKO-APAP mice compared with WT-APAP mice (Fig. 2E). On the other hand, HMGB2 levels were increased in HKO-APAP mice compared with WT-APAP mice (Fig. 2E). Hepatic regeneration and the replacement of necrotic hepatocytes usually follow liver injury to promote tissue mass and recovery. We found that protein expression of proliferating cell nuclear antigen levels, a marker for cell proliferation was increased in WT and HKO mice with APAP overdose which were lower in HKO-APAP mice (Fig. 2F). The reduced cell proliferation was associated with elevated hepatocyte nuclear factor 4-alpha levels, a key transcription factor involved in liver development, which was increased in HKO-APAP mice compared with WT-APAP mice (Fig. 2F), demonstrating that SerpinA3N deficiency could promote liver growth and development in the setting of APAP-induced liver injury. Taken together, hepatocyte SerpinA3N deficiency diminished APAP-induced liver injury and reduced necrosis.

Attenuated Liver Injury in SerpinA3N HKO Mice Is Associated with Reduced Oxidative Damage. The detoxification of NAPQI by GSH is an important aspect in determining the degree of hepatic injury. Levels of GSH were reduced with APAP administration at 12 hours; however, no differences were detected between WT and HKO mice (Fig. 3A), suggesting that SerpinA3N may not modulate APAP metabolism. On the other hand, oxidative damage is known to be induced in mice with APAP overdose, which may contribute to liver injury. Levels of hepatic MDA and H_2O_2 were upregulated in mice with APAP overdose (Fig. 3, B and C) but only liver MDA level was lower in HKO-APAP mice (Fig. 3B). Oxidative stress is generally a result of impaired ability of antioxidant enzymes to clear reactive oxygen species levels within the cells. To determine whether the lower oxidative stress in SerpinA3N HKO mice was associated with alterations in redox balance, we measured several antioxidant enzymes [Catalase, glutathione peroxidase 1 (Gpx1), superoxide dismutase 1 (Sod1), peroxiredoxin-1 (Prdx1)]. No changes were reported on mRNA levels of nuclear factor-like 2 (*Nrf2*), *Catalase*, *Prdx1*, and *Sod1* between WT-APAP and HKP-APAP mice (Fig. 3D), but protein levels of PRDX1 and GPX1 in SerpinA3N HKO-APAP mice were increased compared with WT-APAP mice (Fig. 3E). Additionally, no changes were reported on protein expression of CATALASE or NRF2 between WT-APAP and HKO-APAP mice (Fig. 3E). Protein levels of CYP2E1 were also not altered between groups (Fig. 3E), but *Cyp1a2* mRNA levels were reduced in HKO-APAP mice compared with WT-APAP mice (Fig. 3F). Because antioxidant enzymes arise from mitochondria and mitochondrial dysfunction may be associated with APAP-induced injury, we assessed markers of mitochondrial biogenesis (Fig. 3G). However, no changes were observed between WT and HKO mice on mRNA levels of *Cytochrome C*, *Cox I, Cox II*, and *Cox IV* (Fig. 3G). Interestingly, pyruvate dehydrogenase kinase 4 associated with the mitochondria was lower in HKO-APAP mice compared with WT-APAP mice (Fig. 3H). Taken together, the attenuated liver damage in HKO-APAP mice may be associated with lower oxidative damage because of increased protein levels of several antioxidant enzymes.

Hepatocyte SerpinA3N Deficiency Attenuates APAP-nduced Inflammation and Promotes M2 Macrophage Activation. The inflammatory response after hepatocyte injury plays a crucial role in the pathologic outcome of APAP-induced acute liver failure. In our study, mRNA expression of *F4/80*, a marker for mature macrophages, was higher in SerpinA3N HKO-APAP mice compared with WT-APAP mice (Fig. 4A). This was confirmed by immunohistochemistry staining for F4/80 where higher levels of hepatic macrophages were observed in HKO-APAP mice compared with WT-APAP mice (Fig. 4B). Furthermore, plasma IL-6 levels were markedly induced in response to APAP, but no difference was detected with WT-APAP and HKO-APAP mice (Fig. 4C).

Macrophages can be polarized into two distinct forms, known as M1 proinflammatory or M2 anti-inflammatory depending on the stimuli or physiologic conditions (Sica and Mantovani, 2012). Accordingly, mRNA levels of M1 macrophage markers *IL-6*, *IL-1β*, *Cd68*, *and Cd11c* were diminished in HKO-APAP mice compared with WT-APAP mice (Fig. 4, D and E). Tumor necrosis factor alpha levels were not different between WT-APAP and HKO-APAP mice (Fig. 4D). M2 markers, Arginase-1 and *Cd163,* were upregulated in HKO-APAP mice compared with WT-APAP mice, although *IL-10* levels were reduced (Fig. 4F), suggesting that activation of macrophages in HKO mice may be due to increased M2 rather than M1 macrophages. Serum amyloid A1, an acute phase protein, was increased in HKO-APAP mice compared with WT-APAP mice (Fig. 4F), whereas C-C chemokine receptor type 2 expression was reduced in HKO-APAP mice (Fig. 4F). Collectively, our data demonstrate that SerpinA3N is induced in response to inflammation and that SerpinA3N deficiency can attenuate the inflammatory response by increasing the M2 macrophage phenotype.

Hepatocyte SerpinA3N Deficiency Reduces Neutrophil Accumulation in Mice with APAP Overdose. The accumulation of hepatic neutrophils at the site of injury plays a central role in inflammation to promote regeneration (Ramaiah and Jaeschke, 2007). We found that hepatic *Ly6g,* chemokine (C-X-C motif) ligand (*Cxcl*)-1, *Cxcl2*, and macrophage inflammatory protein-2 mRNA levels were attenuated in HKO-APAP mice compared with WT-APAP mice (Fig. 5, A–C). To acquire an understanding of how SerpinA3N regulates the inflammatory response, signaling pathways related to inflammation were investigated (Fig. 5, D and E). APAP exposure in mice can induce mitochondrial dysfunction and c-Jun N-terminal kinase (JNK) activation, which is involved in hepatocyte cell death. Indeed, JNK activation was induced in response to APAP overdose; however, no differences were observed between WT-APAP and HKO-APAP mice (Fig. 5D). A similar alteration was also observed with c-Jun activation, a downstream effector of JNK (Fig. 5D). Interestingly, p38 phosphorylation was reduced in mice with APAP, compared with PBS-treated group, but HKO-APAP had higher p38 phosphorylation compared with WT-APAP mice (Fig. 5E). Activation of extracellular signal–regulated kinases 1/2 by phosphorylation was similar between WT-APAP and HKO-APAP mice (Fig. 5E).

Activation of 5′ AMP-Activated Protein Kinase–Unc-51-Like Autophagy Activating Kinase 1 Signaling Pathway Diminishes APAP-Induced Liver Injury in Mice with SerpinA3N Deficiency. A single i.p. dose of APAP induced a similar increase in AKT phosphorylation in WT and HKO mice, but no differences were reported in total AKT protein (Fig. 6A). Furthermore, 5′ AMP-activated protein kinase (AMPK) was also upregulated in HKO mice in response to APAP, but phosphorylation was blunted in WT-APAP mice (Fig. 6A). The AKT signaling pathway can regulate the mammalian target of rapamycin (mTOR) signaling pathway that is essential for cell metabolism, proliferation, and survival (Kim et al., 2011). We found that mTOR activation by phosphorylation on the ser2448 residue was attenuated in WT-APAP when compared with HKO-APAP (Fig. 6B).

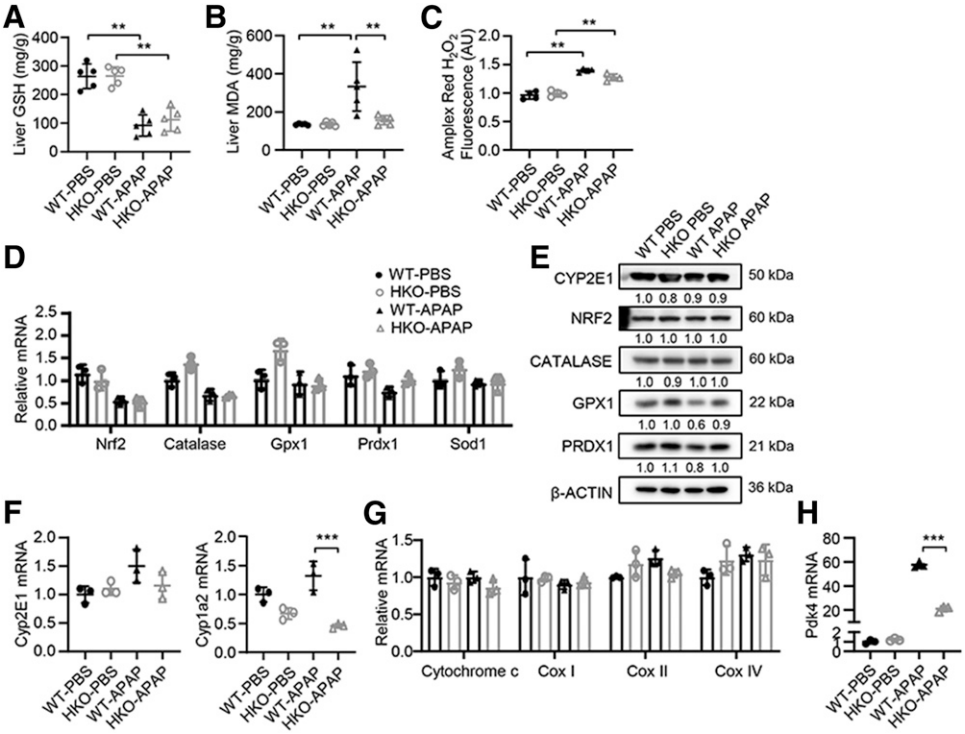

Fig. 3. Hepatocyte SerpinA3N deficiency reduces oxidative stress in mice with APAP overdose. Mice were treated with PBS or APAP (400 mg/kg) for 12 hours. (A–C) Levels of hepatic glutathione (A), MDA (B), and H_2O_2 (C). (D) qPCR analysis of antioxidant enzymes (*Nrf2, Catalase, Gpx1, Prdx1*, and *Sod1*). (E) Immunoblotting for CYP2E1, NRF2, CATALASE, GPX1, PRDX1, and the respective loading control, β-ACTIN. (F–H) qPCR analysis of *Cyp2e1* (F), *Cyp1a2*, mitochondrial genes (*Cytochrome C*, *Cox I,* and *Cox IV*) (G), and pyruvate dehydrogenase kindase-4 (*Pdk4*) (H). Data are presented as means ± S.D., $n = 4$ to 5 per group. $^{**}P < 0.01$ (considered statistically significant) and $^{***}P < 0.005$ (considered statistically significant) after Bonferroni correction compared with drug treatment (A and C) or WT within the same drug treatment (B, F, H).

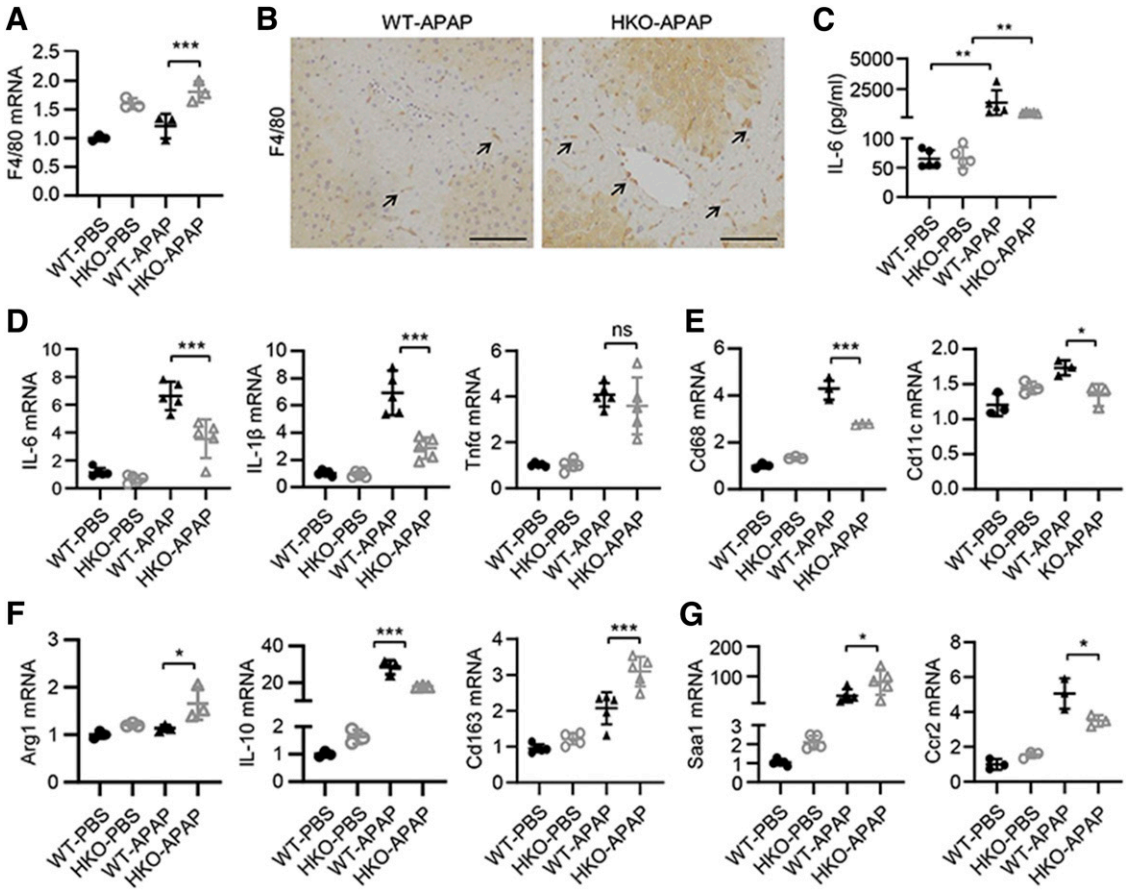

Fig. 4. Hepatocyte SerpinA3N deficiency attenuates hepatic inflammation in mice with APAP overdose. (A) qPCR analysis of hepatic *F4/80* mRNA. (B) Representative images of immunohistochemistry staining for F4/80 in WT-APAP and SerpinA3N HKO-APAP mice. Scale bar, 100 μm. (C) Plasma IL-6 levels. (D–G) qPCR analysis of hepatic mRNA expression of *IL-6*, *IL-1b*, Tumor necrosis factor alpha (*Tnfα*) (D), *Cd68*, *Cd11c* (E), Arginase-1 (*Arg1*), *IL-10*, *Cd163* (F), Serum amyloid A1 (*Saa1*), and C-C chemokine receptor 2 (*Ccr2*) (G). Data are presented as means ± S.D., $n = 5$ per group. $^{*}P < 0.05$; $^{**}P < 0.01$ (considered statistically significant) and $^{***}P < 0.005$ (considered statistically significant) after Bonferroni correction compared with drug treatment (C) or WT within the same drug treatment (A and D–G), respectively.

Similarly, phosphorylation of P70S6K, a downstream mediator of mTOR, was blunted in WT-APAP, compared with that of HKO-APAP, but no differences were observed with total P70S6K levels (Fig. 6B). Raptor and Rictor are associated with mTOR activation (Kim et al., 2002; Sarbassov et al., 2004). We found that RAPTOR protein expression was significantly upregulated in HKO-APAP compared with WT-APAP mice (Fig. 6B).

Autophagy plays an important process in cell development and growth, and compelling evidence demonstrates that autophagy may protect against APAP-induced injury (Igusa et al., 2012; Ni et al., 2012; Lin et al., 2014; Sydor et al., 2017). The initiating step of autophagy involves the unc-51-like autophagy activating kinase 1 (ULK1) complex which is modulated by mammalian target of rapamycin complex 1 (mTORC1) and AMPK (Kim et al., 2011; Mack et al., 2012). We found that APAP-induced liver injury suppressed ULK1 phosphorylation in WT-APAP mice which was upregulated in HKO-APAP mice (Fig. 6C). Additionally, BECLIN1 was lower in WT-APAP mice but was increased in HKO-APAP mice (Fig. 6C). Several autophagy related gene (ATG) proteins, including ATG12 covalently bound ATG5, ATG5, ATG7, ATG12, and ATG16L were reduced in WT mice administered with APAP but were upregulated with SerpinA3N deficiency (Fig. 6C). APAP overdose markedly upregulated p62 protein levels but no differences were reported between WT and HKO mice (Fig. 6C). Taken together, our data indicate that hepatocyte SerpinA3N deficiency may modulate the AMPK-ULK1 signaling pathway to reduce APAP-induced liver injury.

Discussion

Acetaminophen is therapeutically safe at recommended doses; however, severe liver damage may result as a side effect that can have fatal consequences (McGill et al., 2012; Ramachandran and Jaeschke, 2018). Our studies indicate that SerpinA3N has a pathophysiological role in modulating APAP-induced liver injury. More specifically, mice with hepatocyte SerpinA3N deficiency have diminished APAP-induced liver injury, reduced inflammation and neutrophil infiltration which may be associated with autophagy.

Autophagy is a common homeostatic mechanism that occurs in response to diverse stress and physiologic conditions (Ramachandran and Jaeschke, 2018). The activity of autophagy is primarily controlled by the counter-regulatory effects of nutrient sensing kinases, mTOR and AMPK, leading to the formation of light chain (LC3) autophagosomes (Kim et al., 2011; Nwadike et al., 2018). Several studies have demonstrated that autophagy can protect against APAP-induced

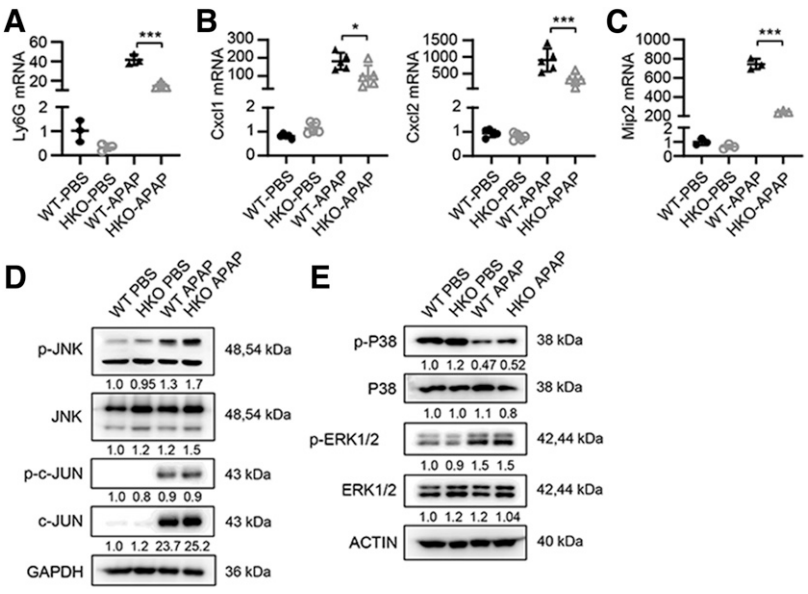

Fig. 5. Hepatocyte SerpinA3N deficiency reduces neutrophil accumulation in mice with APAP overdose. (A–C) qPCR analysis of hepatic mRNA expression of *Ly6G* (A), *Cxcl1*, *Cxcl2* (B), and macrophage inflammatory protein-2 (*Mip2*) (C). Data are presented as means ± S.D., $n = 5$ per group. $^{*}P < 0.05$; $^{***}P < 0.005$ (considered statistically significant) after Bonferroni correction compared with WT within the same drug treatment (A–C). (D, E) Immunoblotting for JNKs (D) and p38 mitogen-activated protein kinases (MAPKs) and extracellular signal–regulated protein kinases (ERKs) (E), and the respective loading control, glyceraldehyde-3-phosphate dehydrogenase (GAPDH). p-, phosphorylated.

injury (Igusa et al., 2012; Ni et al., 2012; Lin et al., 2014; Sydor et al., 2017). Of note, autophagy limits inflammatory cytokine maturation, whereas inhibition of autophagy further exacerbates liver injury and necrosis (Ilyas et al., 2016; Lalazar et al., 2016; Ni et al., 2016). The improvement in liver injury in response to APAP in our SerpinA3N deficient mice may be through the positive regulation of the AMPK signaling pathway. However, autophagy is an intricate process that is associated with many regulators, including several modifications on the ULK1 site (Lee et al., 2010; Roach, 2011; Mack et al., 2012). Our study showed that SerpinA3N deficient mice upregulated ser555 phosphorylation of ULK1 which suggests that autophagy may be involved to promote autophagosome formation. However, it is important to note that

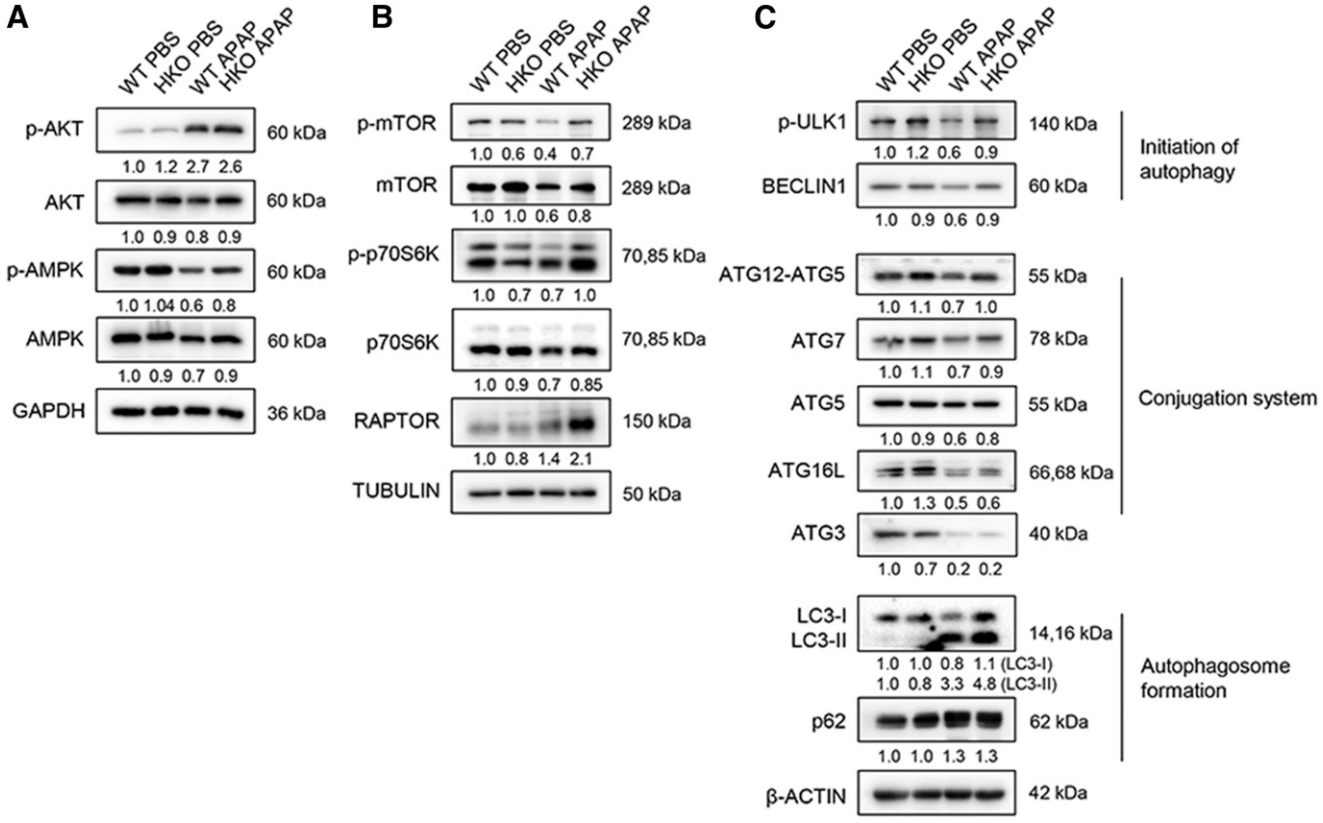

Fig. 6. Hepatocyte SerpinA3N deficiency modulates AMPK-ULK signaling pathway to reduce APAP-induced liver injury. Immunoblotting for AKT-AMPK pathway (A), mTOR pathway (B), and markers of autophagy (p-ULK1, BECLIN1, ATG3, ATG5, ATG7, ATG12-ATG5, ATG16L, LC3-I, LC3-II, and p62) (C) plus the respective loading controls, glyceraldehyde-3-phosphate dehydrogenase (GAPDH), TUBULIN, and β-ACTIN. p-, phosphorylated.

additional autophagy experiments including assessment of autophagosome quantification, LC3 binding protein turnover and autophagic flux are required to ascertain the involvement of autophagy in ameliorating APAP-induced liver injury in SerpinA3N knockout mice.

It is worth noting that mTOR phosphorylation was markedly upregulated in SerpinA3N HKO mice with APAP administration compared with WT-APAP mice, and similarly its downstream molecule phosphorylated P70S6K was also significantly induced. Our findings coincide with a recent study demonstrating that SerpinA3N expression in skeletal muscle and C2C12 cells were increased after mTOR inactivation (Gueugneau et al., 2018). Our findings are in accordance with the abovementioned study suggesting that mTOR may serve as a negative regulator of SerpinA3N in APAP-induced hepatotoxicity. Furthermore, in contrast to the proinflammatory effect of mTORC2, mTORC1 favors, to some extent, an anti-inflammatory macrophage polarization that is protective against inflammation. Indeed, our studies demonstrate that the higher levels of macrophages found in HKO mice showed increased M2-like phenotype. However, additional assessment between mTORC1 (by Raptor phosphorylation) and mTORC2 (by Rictor phosphorylation) is required to provide a definitive conclusion on the role of mTOR in this study.

Interestingly, F4/80 levels were higher in SerpinA3N HKO mice, which were not further induced with APAP administration. Consistent with this, Cd163, a cell marker from the monocyte/macrophage lineage was also elevated in APAP-induced mice which was further enhanced in HKO mice. This would suggest that increased macrophage activation would correlate with a proinflammatory response; however, mice with SerpinA3N deficiency had lower levels of inflammatory cytokines (IL-6, IL-1β, Cd68, and Cd11c). The primary function of SerpinA3N is to bind to specific proteases to limit inflammation related damage, suggesting that SerpinA3N may have an anti-inflammatory response. However, our study reported that WT mice with intact SerpinA3N expression had increased inflammation with concomitant liver injury.

On the contrary, the reduced inflammatory response in hepatocyte SerpinA3N HKO mice was associated with increased macrophage induction. This contradictory finding suggests that there may be some form of compensatory effect that may be related to the ablation of SerpinA3N in hepatocytes. SerpinA3N is mainly synthesized in the liver, so it is not surprising that other hepatic cell types may be involved, particularly Kupffer cells or stellate cells. Indeed, macrophages have been shown to express the SERPINA3 protein in the hypothalamus under pathologic conditions (Montesinos-Rongen et al., 2008). In the current study, we did not assess SerpinA3N levels in Kupffer cells. However, it is possible that macrophage activation and SerpinA3N levels could be increased to compensate for the ablated SerpinA3N expression in hepatocytes, as a compensatory consequence. Future studies measuring SerpinA3N levels in other hepatic cell types are warranted to determine what the specific roles of each cell type account for. Additionally, studies should identify whether the additional loss of SerpinA3N in Kupffer cells and hepatocytes (using a double knockout model) provides protection or has deleterious effects against APAP-induced hepatic injury. Finally, it may be possible that one of the SerpinA3 members, which are all similar to SerpinA3N, would likely compensate and therefore ideally the complete loss of function of the whole SerpinA3 members may be worth considering.

In summary, our study suggests that SerpinA3N may be a regulator in APAP-induced hepatotoxicity and inflammation. Finally, our study may offer novel insights into therapeutic options to target SerpinA3N to treat APAP-induced liver injury.

Authorship Contributions

Participated in research design: Tran.
Conducted experiments: Tran, Wu, Wang, Shin.
Performed data analysis: Tran, Shin.
Wrote or contributed to the writing of the manuscript: Tran, Shin.

References

Aslam MS and Yuan L (2020) Serpina3n: potential drug and challenges, mini review. *J Drug Target* **28**:368–378.

Cao LL, Pei XF, Qiao X, Yu J, Ye H, Xi CL, Wang PY, and Gong ZL (2018) SERPINA3 Silencing inhibits the migration, invasion, and liver metastasis of colon cancer cells. *Dig Dis Sci* **63**:2309–2319.

Dalby MJ, Aviello G, Ross AW, Walker AW, Barrett P, and Morgan PJ (2018) Diet induced obesity is independent of metabolic endotoxemia and TLR4 signalling, but markedly increases hypothalamic expression of the acute phase protein, SerpinA3N. *Sci Rep* **8**:15648.

Gueugneau M, d'Hose D, Barbé C, de Barsy M, Lause P, Maiter D, Bindels LB, Delzenne NM, Schaeffer L, Gangloff YG, et al. (2018) Increased Serpina3n release into circulation during glucocorticoid-mediated muscle atrophy. *J Cachexia Sarcopenia Muscle* **9**:929–946.

Haile Y, Carmine-Simmen K, Olechowski C, Kerr B, Bleackley RC, and Giuliani F (2015) Granzyme B-inhibitor serpina3n induces neuroprotection in vitro and in vivo. *J Neuroinflammation* **12**:157.

Hinson JA, Roberts DW, and James LP (2010) Mechanisms of acetaminophen-induced liver necrosis. *Handb Exp Pharmacol* **196**:369–405.

Horvath AJ, Irving JA, Rossjohn J, Law RH, Bottomley SP, Quinsey NS, Pike RN, Coughlin PB, and Whisstock JC (2005) The murine orthologue of human antichymotrypsin: a structural paradigm for clade A3 serpins. *J Biol Chem* **280**: 43168–43178.

Hsu I, Parkinson LG, Shen Y, Toro A, Brown T, Zhao H, Bleackley RC, and Granville DJ (2014) Serpina3n accelerates tissue repair in a diabetic mouse model of delayed wound healing. *Cell Death Dis* **5**:e1458.

Igusa Y, Yamashina S, Izumi K, Inami Y, Fukada H, Komatsu M, Tanaka K, Ikejima K, and Watanabe S (2012) Loss of autophagy promotes murine acetaminophen hepatotoxicity. *J Gastroenterol* **47**:433–443.

Ilyas G, Zhao E, Liu K, Lin Y, Tesfa L, Tanaka KE, and Czaja MJ (2016) Macrophage autophagy limits acute toxic liver injury in mice through down regulation of interleukin-1β. *J Hepatol* **64**:118–127.

Kalsheker N, Morley S, and Morgan K (2002) Gene regulation of the serine proteinase inhibitors alpha1-antitrypsin and alpha1-antichymotrypsin. *Biochem Soc Trans* **30**:93–98.

Kim DH, Sarbassov DD, Ali SM, King JE, Latek RR, Erdjument-Bromage H, Tempst P, and Sabatini DM (2002) mTOR interacts with raptor to form a nutrient-sensitive complex that signals to the cell growth machinery. *Cell* **110**:163–175.

Kim J, Kundu M, Viollet B, and Guan KL (2011) AMPK and mTOR regulate autophagy through direct phosphorylation of Ulk1. *Nat Cell Biol* **13**:132–141.

Ko E, Kim JS, Bae JW, Kim J, Park SG, and Jung G (2019) SERPINA3 is a key modulator of HNRNP-K transcriptional activity against oxidative stress in HCC. *Redox Biol* **24**:101217.

Ko E, Seo HW, Jung ES, Ju S, Kim BH, Cho H, Kim YJ, Park YM, Kim JS, and Jung G (2018) PI3Kδ is a therapeutic target in hepatocellular carcinoma. *Hepatology* **68**: 2285–2300.

Lalazar G, Ilyas G, Malik SA, Liu K, Zhao E, Amir M, Lin Y, Tanaka KE, and Czaja MJ (2016) Autophagy confers resistance to lipopolysaccharide-induced mouse hepatocyte injury. *Am J Physiol Gastrointest Liver Physiol* **311**:G377–G386.

Lee JW, Park S, Takahashi Y, and Wang HG (2010) The association of AMPK with ULK1 regulates autophagy. *PLoS One* **5**:e15394.

Lin Z, Wu F, Lin S, Pan X, Jin L, Lu T, Shi L, Wang Y, Xu A, and Li X (2014) Adiponectin protects against acetaminophen-induced mitochondrial dysfunction and acute liver injury by promoting autophagy in mice. *J Hepatol* **61**:825–831.

Mack HID, Zheng B, Asara JM, and Thomas SM (2012) AMPK-dependent phosphorylation of ULK1 regulates ATG9 localization. *Autophagy* **8**:1197–1214.

Matsuzaki S, Iwamura K, Itakura M, Kamiguchi H, and Katsunuma T (1981) A clinical evaluation of serum alpha-1-antichymotrypsin levels in liver disease and cancers. *Gastroenterol Jpn* **16**:582–591.

McGill MR and Jaeschke H (2013) Metabolism and disposition of acetaminophen: recent advances in relation to hepatotoxicity and diagnosis. *Pharm Res* **30**: 2174–2187.

McGill MR, Sharpe MR, Williams CD, Taha M, Curry SC, and Jaeschke H (2012) The mechanism underlying acetaminophen-induced hepatotoxicity in humans and mice involves mitochondrial damage and nuclear DNA fragmentation. *J Clin Invest* **122**: 1574–1583.

Montesinos-Rongen M, Brunn A, Bentink S, Basso K, Lim WK, Klapper W, Schaller C, Reifenberger G, Rubenstein J, Wiestler OD, et al. (2008) Gene expression profiling suggests primary central nervous system lymphomas to be derived from a late germinal center B cell. *Leukemia* **22**:400–405.

Morgan K and Kalsheker NA (1997) Regulation of the serine proteinase inhibitor (SERPIN) gene α 1-antitrypsin: a paradigm for other SERPINs. *Int J Biochem Cell Biol* **29**:1501–1511.
Ni HM, Bockus A, Boggess N, Jaeschke H, and Ding WX (2012) Activation of autophagy protects against acetaminophen-induced hepatotoxicity. *Hepatology* **55**: 222–232.
Ni HM, McGill MR, Chao X, Du K, Williams JA, Xie Y, Jaeschke H, and Ding WX (2016) Removal of acetaminophen protein adducts by autophagy protects against acetaminophen-induced liver injury in mice. *J Hepatol* **65**:354–362.
Nwadike C, Williamson LE, Gallagher LE, Guan J-L, and Chan EYW (2018) AMPK inhibits ULK1-dependent autophagosome formation and lysosomal acidification via distinct mechanisms. *Mol Cell Biol* **38**:e00023-e18.
Ohkawa H, Ohishi N, and Yagi K (1979) Assay for lipid peroxides in animal tissues by thiobarbituric acid reaction. *Anal Biochem* **95**:351–358.
Ramachandran A and Jaeschke H (2018) Acetaminophen toxicity: novel insights into mechanisms and future perspectives. *Gene Expr* **18**:19–30.
Ramaiah SK and Jaeschke H (2007) Role of neutrophils in the pathogenesis of acute inflammatory liver injury. *Toxicol Pathol* **35**:757–766.
Roach PJ (2011) AMPK -> ULK1 -> autophagy. *Mol Cell Biol* **31**:3082–3084.
Sarbassov DD, Ali SM, Kim DH, Guertin DA, Latek RR, Erdjument-Bromage H, Tempst P, and Sabatini DM (2004) Rictor, a novel binding partner of mTOR, defines a rapamycin-insensitive and raptor-independent pathway that regulates the cytoskeleton. *Curr Biol* **14**:1296–1302.
Sergi D, Campbell FM, Grant C, Morris AC, Bachmair EM, Koch C, McLean FH, Muller A, Hoggard N, de Roos B, et al. (2018) *SerpinA3N* is a novel hypothalamic gene upregulated by a high-fat diet and leptin in mice. *Genes Nutr* **13**:28.
Sica A and Mantovani A (2012) Macrophage plasticity and polarization: in vivo veritas. *J Clin Invest* **122**:787–795.
Sydor S, Manka P, Best J, Jafoui S, Sowa JP, Zoubek ME, Hernandez-Gea V, Cubero FJ, Kälsch J, Vetter D, et al. (2017) Krüppel-like factor 6 is a transcriptional activator of autophagy in acute liver injury. *Sci Rep* **7**:8119.
Tjondrokoesoemo A, Schips T, Kanisicak O, Sargent MA, and Molkentin JD (2016) Genetic overexpression of Serpina3n attenuates muscular dystrophy in mice. *Hum Mol Genet* **25**:1192–1202.
Vicuña L, Strochlic DE, Latremoliere A, Bali KK, Simonetti M, Husainie D, Prokosch S, Riva P, Griffin RS, Njoo C, et al. (2015) The serine protease inhibitor SerpinA3N attenuates neuropathic pain by inhibiting T cell-derived leukocyte elastase. *Nat Med* **21**:518–523.
Waise TMZ, Toshinai K, Naznin F, NamKoong C, Md Moin AS, Sakoda H, and Nakazato M (2015) One-day high-fat diet induces inflammation in the nodose ganglion and hypothalamus of mice. *Biochem Biophys Res Commun* **464**: 1157–1162.
Yan M, Huo Y, Yin S, and Hu H (2018) Mechanisms of acetaminophen-induced liver injury and its implications for therapeutic interventions. *Redox Biol* **17**:274–283.

Address correspondence to: Melanie Tran, Department of Physiology, 75 North Eagleville Rd., U-3156, Storrs, CT 06269. E-mail: metran@uchc.edu; or Dong-Ju Shin, Department of Physiology and Neurobiology, 75 North Eagleville Rd., U-3156, Storrs, CT 06269. E-mail: dong-ju.shin@uconn.edu